

Electronic Supplementary Information

Vertically grown nanowire crystals of dibenzotetrathienocoronene (DBTTC) on large-area graphene

B. Kim,^{a†} C. –Y. Chiu,^{b†} S. –J. Kang,^c K. S. Kim,^d G. –H. Lee,^e Z. Chen,^f S. Ahn,^g K. G. Yager,^h J. Ciston,ⁱ C. Nuckolls,^j and
T. Schiros^k

^a Department of Chemistry, New Jersey City University, Jersey City, NJ 07305, USA

^b PPG Industris Inc., Monroeville Chemicals Center, Monroeville, PA 15146 USA

^c School of Energy and Chemical Engineering, Ulsan National Institute of Science and Technology, Ulsan 608-798, South Korea

^d Department of Physics and Graphene Research Institute, Sejong University, Seoul 143-747, South Korea

^e Department of Material Science and Engineering, Yonsei University, Seoul 120-740, South Korea

^f Department of Chemistry, Emory University, Atlanta, GA 30322, USA

^g Soft Innovative Materials Research Center, University of Science and Technology, Daejeon 305-350, South Korea

^h Center for Functional Materials, Brookhaven National Laboratory, Upton, NY 11973, USA

ⁱ Materials Sciences Division, Lawrence Berkeley National Laboratory, Berkeley, CA 94720, USA

^j Department of Chemistry, Columbia University, New York, NY 10027, USA

^{k, a} Materials Research Science and Engineering (MRSEC), Columbia University, New York, NY 10027, USA; ^bFashion Institute of Technology | State University
of New York, New York, NY 10001, USA

† These authors equally contributed to this work.

‡ Electronic Supplementary Information (ESI) available: Surface characterization data, details of GIXD data See DOI: 10.1039/x0xx00000x

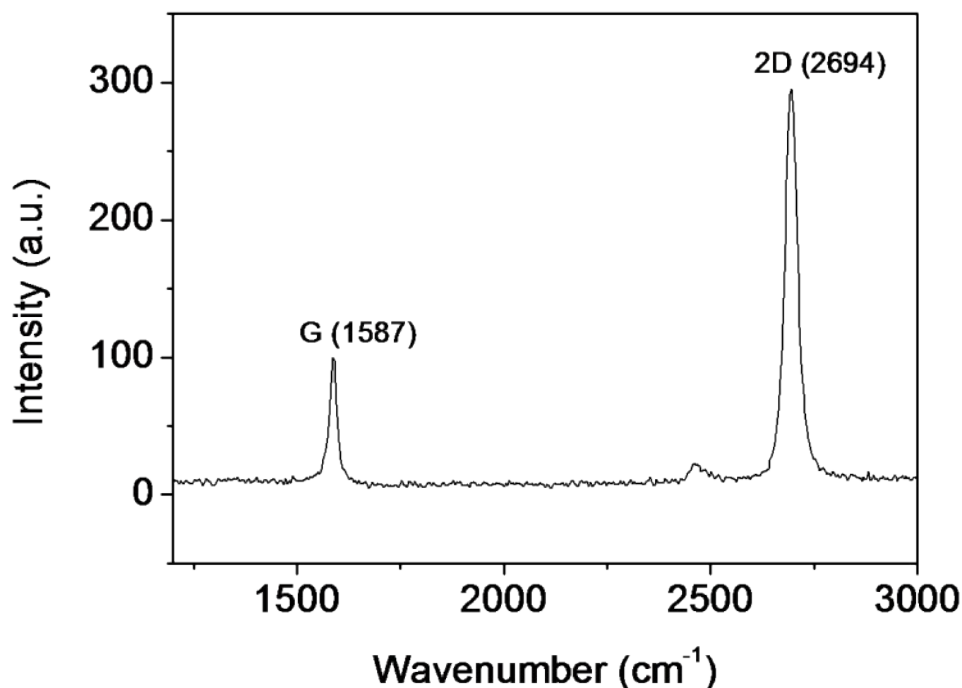


Fig. S1 Raman spectrum of CVD grown graphene film

GIXD

We use X-ray diffraction with an area detector in two sample geometries to obtain morphological and crystallographic information about the DBTTC crystals grown on graphene. Appropriately combining intensity from two measurements, one taken at grazing incidence and another taken in a geometry satisfying the local specular condition for a given Bragg peak (shown in Figure S2 and S3), removes the distortion of the diffraction intensity detected by the flat 2-D area detector image plate in the grazing incidence geometry (Baker, Mannsfeld). The combined 2-D reciprocal (Q-) space diffraction images (Figure S4) and intensity vs. chi plots (Figure S5) accurately represent the substrate-relative orientation of the lattice plane periodicity for the peaks identified and provides a complete 3-D picture of the molecular packing. Using this procedure we find that the dominant pi-stacking direction of the primary vertical DBTTC crystals is perpendicular to the graphene surface for all samples. In addition, we also identify a fraction of crystals with the DBTTC molecules pi-stacked at a narrow range of well-defined angles slightly off from the vertical axis. This is consistent, at the ensemble level, with the vertical and tilted rod-like crystals observed with SEM. While the situation is less clear with regard to packing of molecular columns, we observe peaks corresponding to the that the (01-1) and (010) lattice planes ($q \sim 0.54 \text{ \AA}^{-1}$), which are oriented parallel to the molecular columns have significant and well-defined intensity along the q_e axis. This indicates that the packing of the molecular columns that comprise the primary crystals repeats in-plane, consistent with vertical pi-stacking. However, a fairly isotropic distribution of the molecular columns, which we attribute the residual, more poorly defined crystals from the early stages of growth, are also present in varying proportion across the samples.

(11-1) plane; reflection at $Q=1.7506 \text{ \AA}^{-1}$

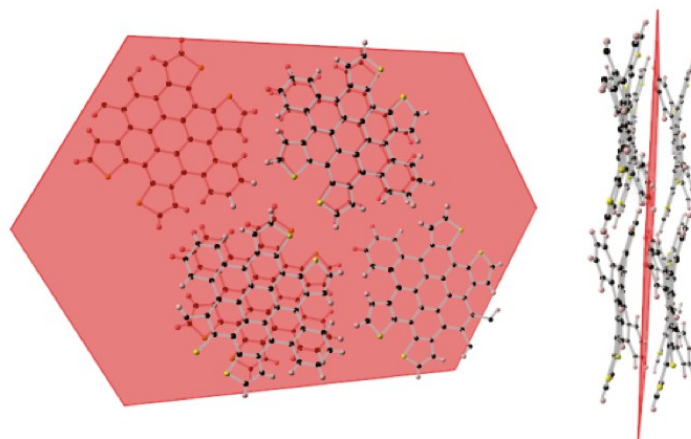


Fig. S2 Relationship between the (11-1) plane of the DBTTC crystal (red hexagon); the [11-1] direction corresponds to the p-stacking direction along the axis of the vertical DBTTC nanowires.

(10-1) $Q=1.6837 \text{ \AA}^{-1}$

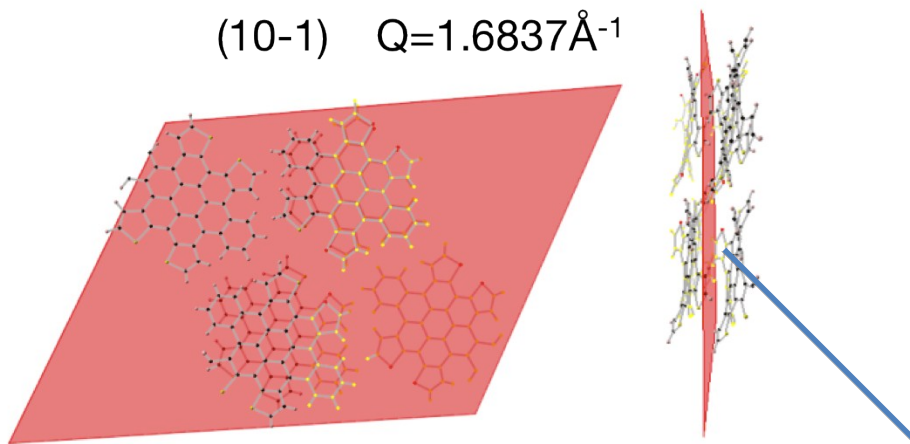


Fig. S3 Relationship between the (10-1) plane of the DBTTC crystal (red parallelogram). Like the [11-1] direction (Figure S2), the [10-1] direction corresponds to the p-stacking direction along the axis of the vertical DBTTC nanowires.

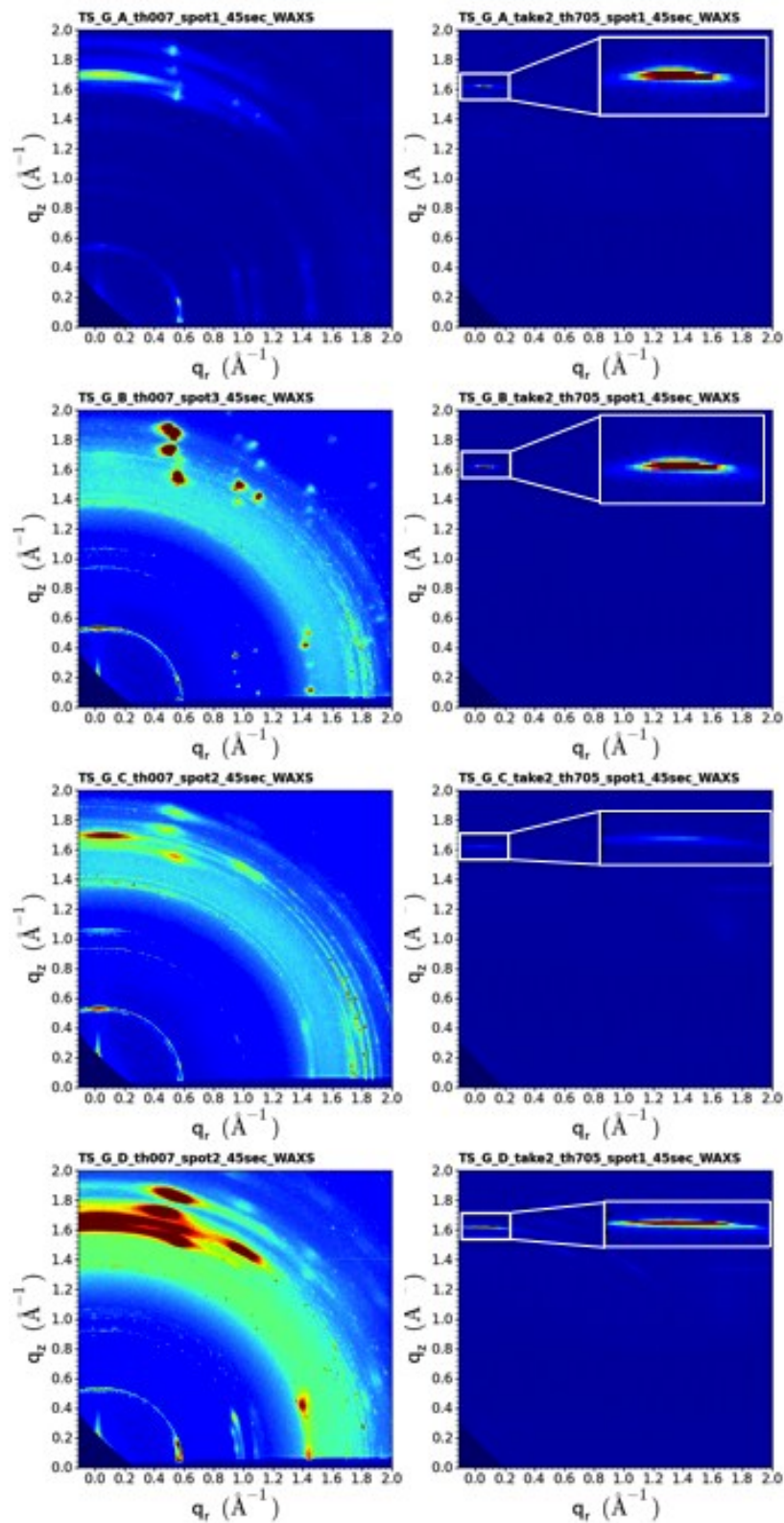


Fig. S4 2-D GIXD patterns of DBTTC/graphene measured in: grazing incidence ($\alpha=0.07^\circ$) (left) and local specular condition for the (11-1) reflection, ($\alpha = \theta_{\text{Bragg}} \sim 7^\circ$) shown in Figure S2.

Intensity vs. chi along $Q=1.74\text{\AA}^{-1}$ ((11-1))

grazing incidence: $\alpha=0.07^\circ$ ($< \theta_{\text{crit}}$)

local specular $\alpha=\theta_{\text{Bragg}}$ for (11-1) $\sim 7^\circ$

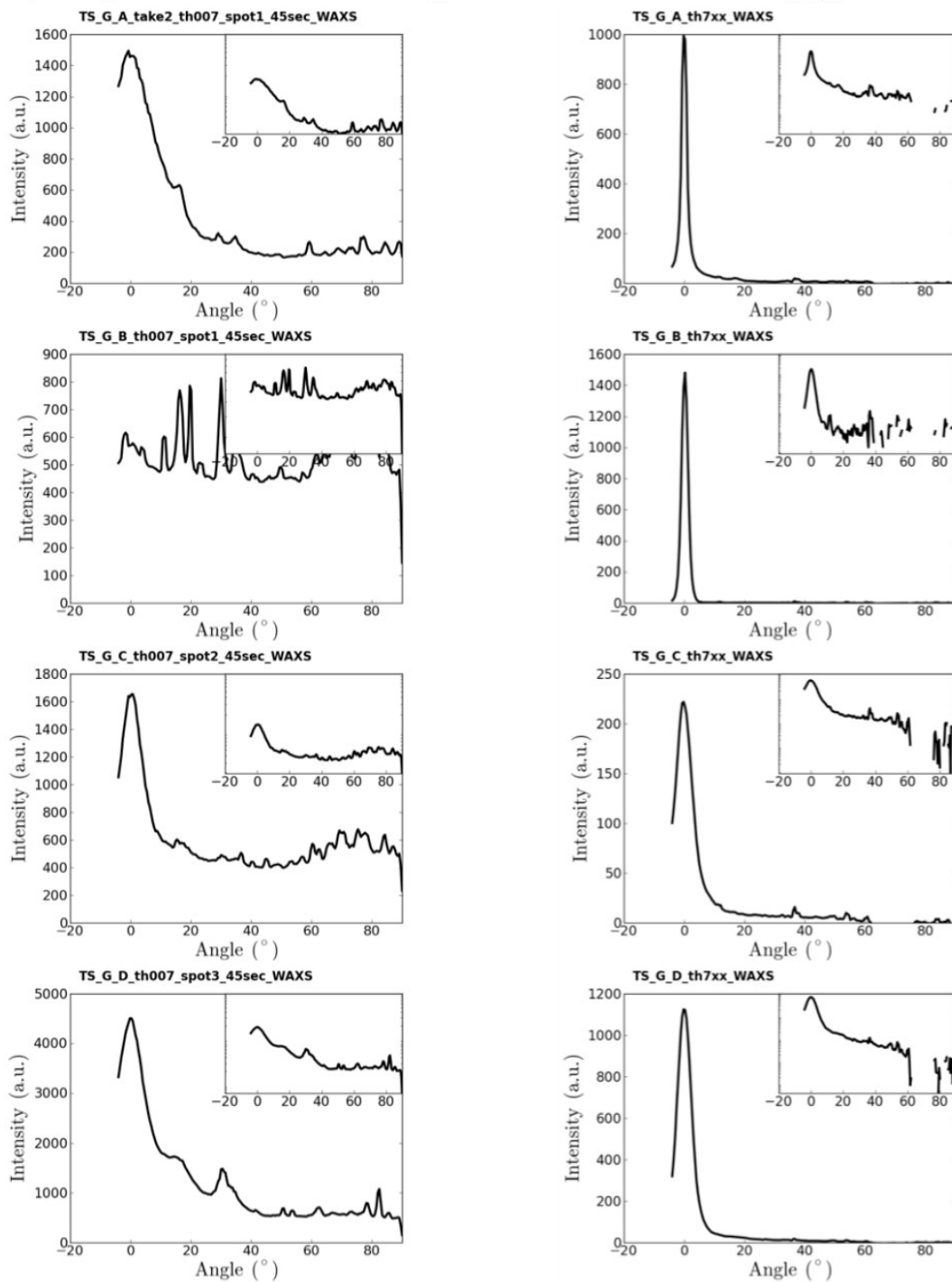


Fig. S5 Intensity vs. Chi for the 2-D diffraction patterns shown in Figure S4 for DBTTC/graphene measured in: grazing incidence ($\alpha=0.07^\circ$) (left) and local specular ($\alpha = \theta_{\text{Bragg}} \sim 7^\circ$).



Fig. S6 DBTTC crystals grown on mica film

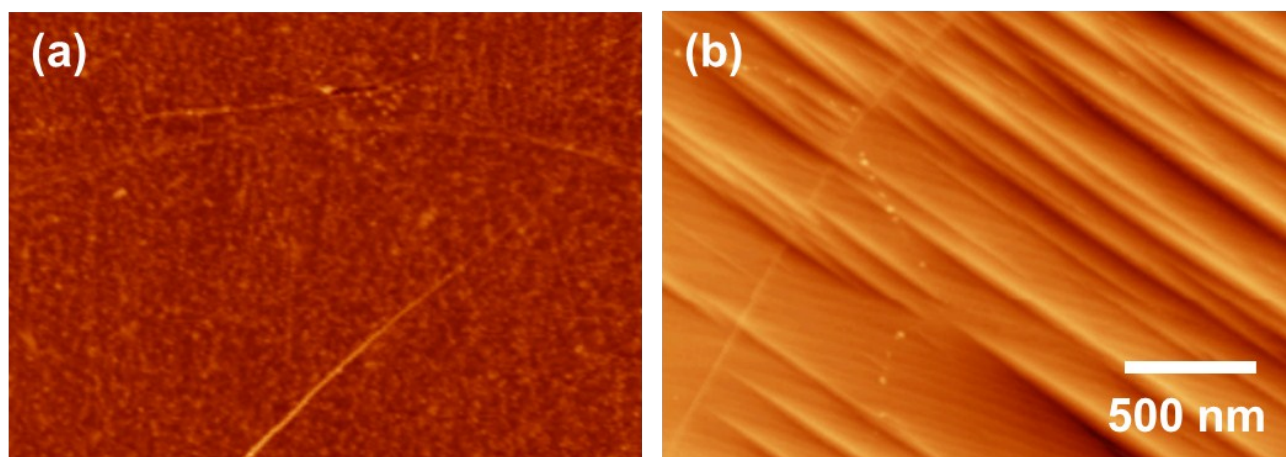


Fig. S7 AFM images of (a) graphene transferred to SiO₂ surface, (b) graphene grown copper foil, and (c) highly-oriented pyrolytic graphite.

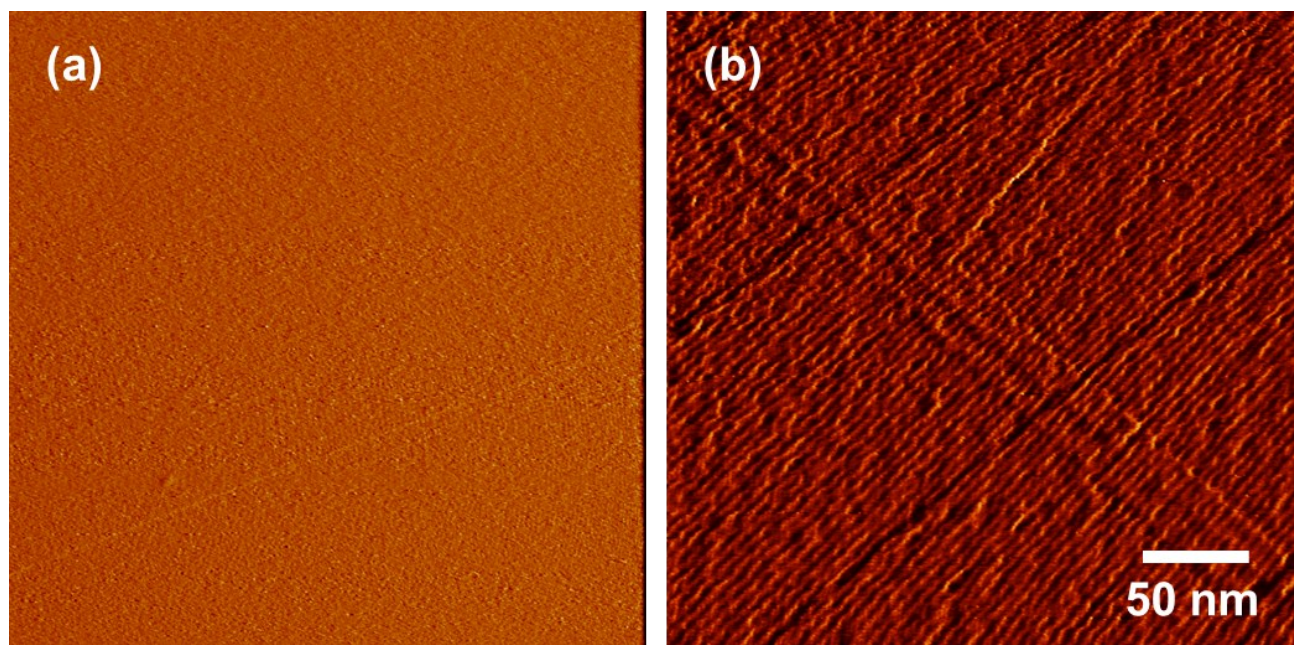


Fig. S8 STM images of (a) HOPG and (b) graphene grown on copper foil.

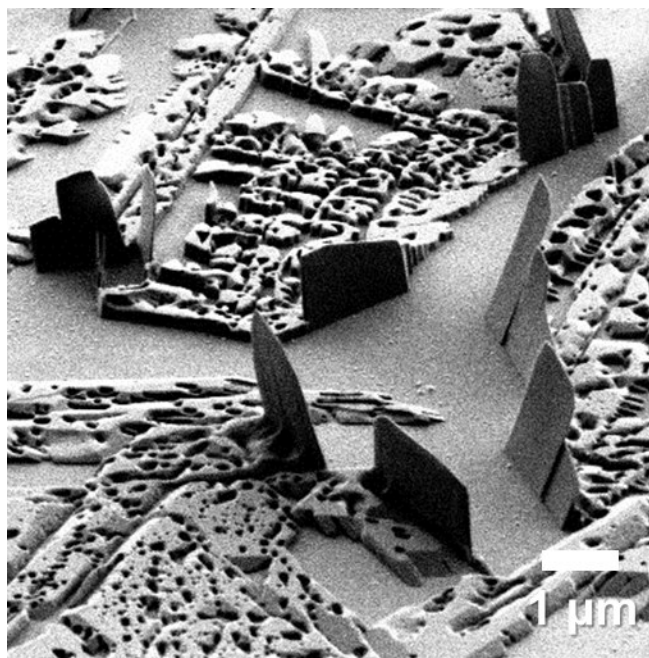


Fig. S9 SEM image of DBTTC crystal growth (340 °C, 200 SCCM, 2 mg of DBTTC) on HOPG for 8 hours.

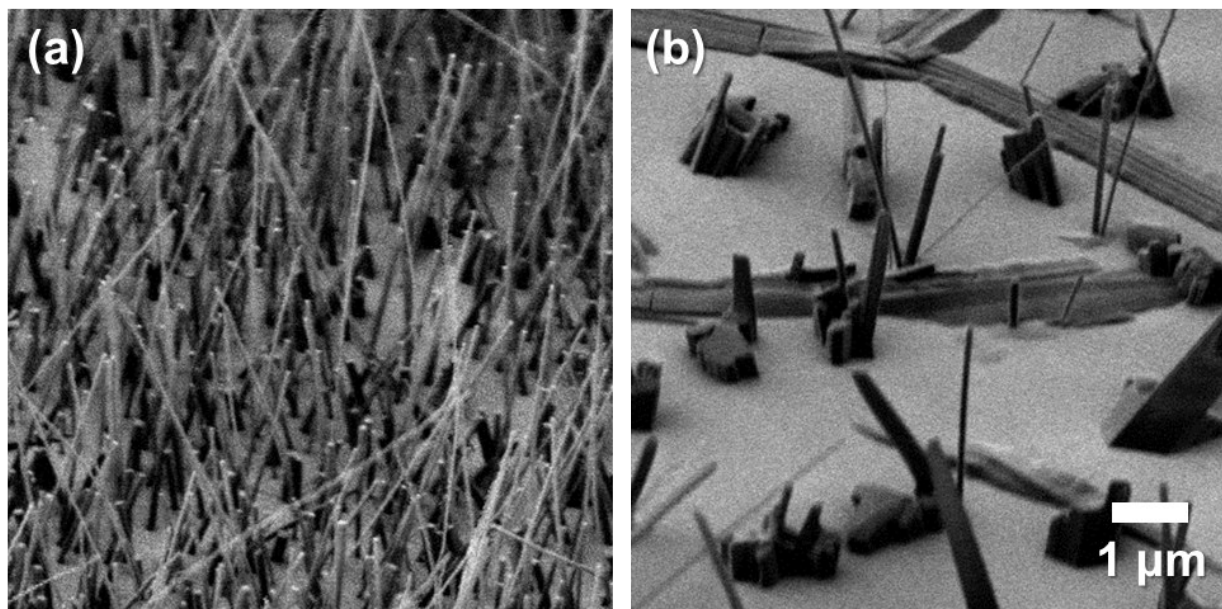


Fig. S10 SEM images of DBTTC growth (340 °C, 200 SCCM, 2 mg of DBTTC) (a) on graphene/SiO₂ substrate using ammonium persulfate etchant and (b) on graphene/SiO₂ substrate using ammonium persulfate etchant with 1 nm thin film of Fe.

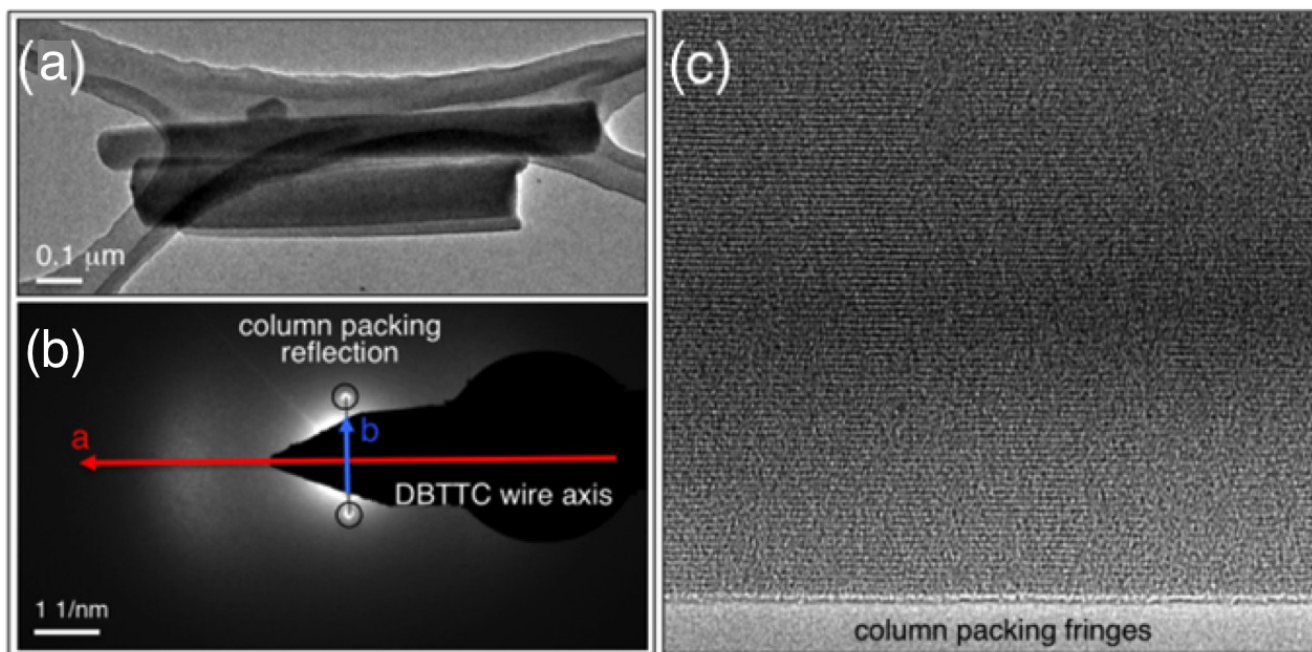


Fig. S11 (a) Bright field image and (b) SAED of DBTTC crystals after long exposure of electron beam and (c) column packing fringes of a DBTTC crystal.